

[CH]

Sr-Nd-Pb isotopic evolution of Gran Canaria: evidence for shallow enriched mantle beneath the Canary Islands

Kaj Hoernle ^{a,1}, George Tilton ^a and Hans-Ulrich Schmincke ^b

^a Department of Geological Sciences, University of California, Santa Barbara, CA 93106, USA

^b GEOMAR, Wischhofstrasse 1-3, D-2300 Kiel-14, Germany

Received July 24, 1990; revised version accepted June 13, 1991

ABSTRACT

We report the Sr, Nd and Pb isotopic compositions (1) of 66 lava flows and dikes spanning the circa 15 Myr subaerial volcanic history of Gran Canaria and (2) of five Miocene through Cretaceous sediment samples from DSDP site 397, located 100 km south of Gran Canaria. The isotope ratios of the Gran Canaria samples vary for $^{87}\text{Sr}/^{86}\text{Sr}$: 0.70302–0.70346, for $^{143}\text{Nd}/^{144}\text{Nd}$: 0.51275–0.51298, and for $^{206}\text{Pb}/^{204}\text{Pb}$: 18.76–20.01. The Miocene and the Pliocene–Recent volcanics form distinct trends on isotope correlation diagrams. The most SiO_2 -undersaturated volcanics from each group have the least radiogenic Sr and most radiogenic Pb, whereas evolved volcanics from each group have the most radiogenic Sr and least radiogenic Pb. In the Pliocene–Recent group, the most undersaturated basalts also have the most radiogenic Nd, and the evolved volcanics have the least radiogenic Nd. The most SiO_2 -saturated basalts have intermediate compositions within each age group. Although the two age groups have overlapping Sr and Nd isotope ratios, the Pliocene–Recent volcanics have less radiogenic Pb than the Miocene volcanics.

At least four components are required to explain the isotope systematics of Gran Canaria by mixing. There is no evidence for crustal contamination in any of the volcanics. The most undersaturated Miocene volcanics fall within the field for the two youngest and westernmost Canary Islands in all isotope correlation diagrams and thus appear to have the most plume-like (high $^{238}\text{U}/^{204}\text{Pb}$) HIMU-like composition. During the Pliocene–Recent epochs, the plume was located to the west of Gran Canaria. The isotopic composition of the most undersaturated Pliocene–Recent volcanics may reflect entrainment of asthenospheric material (with a depleted mantle (DM)-like composition), as plume material was transported through the upper asthenosphere to the base of the lithosphere beneath Gran Canaria. The shift in isotopic composition with increasing SiO_2 -saturation in the basalts and degree of differentiation for all volcanics is interpreted to reflect assimilation of enriched mantle (EM1 and EM2) (cf. [1]) in the lithosphere beneath Gran Canaria. This enriched mantle may have been derived from the continental lithospheric mantle beneath the West African Craton by thermal erosion or delamination during rifting of Pangaea. This study suggests that the enriched mantle components (EM1 and EM2) may be stored in the shallow mantle, whereas the HIMU component may have a deeper origin.

1. Introduction

In recent years, there has been an explosion in the amount of Sr-Nd-Pb isotope data from ocean islands. At least four components are required to explain the range in the ocean island Sr-Nd-Pb basalt (OIB) data [1]. These are depleted mantle (DM), high- μ ($^{238}\text{U}/^{204}\text{Pb}$) mantle (HIMU), and two enriched mantle components (EM1 and EM2). The location of these components in the mantle

remains a topic of conjecture— i.e., whether they reside in the lithosphere, asthenosphere and/or mantle plumes. Knowledge of the location and distribution of these components, however, is crucial in understanding their origin. Although mantle xenoliths in OIB could potentially provide important information about the composition of the oceanic lithosphere, the xenoliths are almost always found in the highly SiO_2 -undersaturated basalts erupted during the latest evolutionary stages of ocean island volcanism. Therefore, even if the xenoliths have not re-equilibrated with the host basalts, the original isotopic composition of

¹ Present address: Department of Earth Sciences; University of California; Santa Cruz, CA 95064, USA.

the xenoliths may have been significantly altered by interaction with the magmas that form the island [2].

In order to define and to constrain the location of the different isotopic endmembers observed in the Canary Islands, we have undertaken a detailed isotopic study of well-documented volcanic rocks from Gran Canaria. In addition to age constraints, major and trace element data are available on all of the samples [3,4,5 and references therein]. Together with the 36 ignimbrites and lava flows from the upper Hogarzales, Mogan and lower Fataga Formations (ca. 14.1–12.5 Ma) studied by Cou-

sens et al. [6], the 66 samples from lava flows and dikes in this study provide one of the most detailed data sets on a single volcano. The variation in isotope ratios with age, degree of differentiation, SiO₂-saturation in the basalts, and magma production rates constrain the composition of the lithosphere, asthenosphere and the plume beneath the Canary Islands.

2. General geology

The 600 km long Canary Island chain sits on the continental rise (Fig. 1), adjacent to the lower

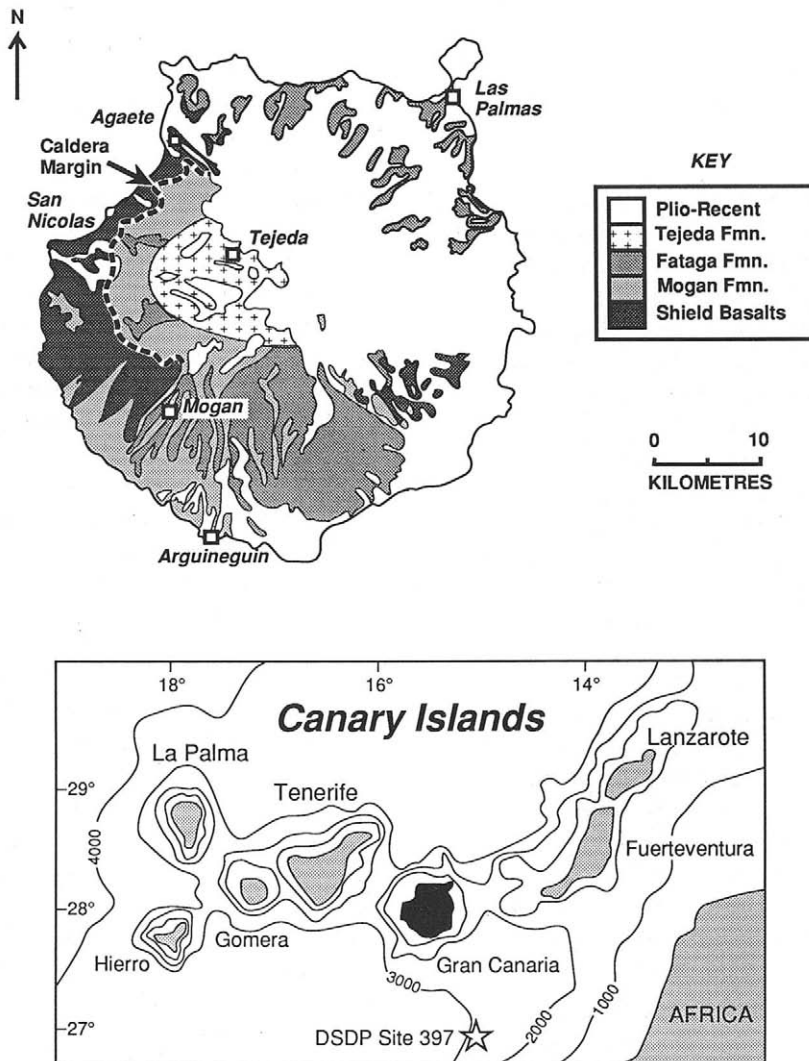


Fig. 1. Geologic map of Gran Canaria with an inset map of the Canary Islands [4].

Proterozoic to Archean (1.8–3.4 Ga) West African Craton [7]. Gran Canaria, the third most easterly island, is located 150 km from the West African continental margin. Seismic refraction studies indicate that up to 10 km of sediments may underlie the easternmost islands. Igneous oceanic crust underlies at least Gran Canaria and the western islands [7,8]. Based on the magnetic anomalies to the north, the age of the oceanic crust beneath the Canary Islands probably ranges from 160 to 180 Ma [9]. While each Island, except Gomera, has had volcanic activity within the last 5000 yr [9], the age of the oldest subaerially exposed volcanics on each island decreases from east (30–80 Ma) to west (2–4 Ma) [10,11], consistent with a hotspot origin for the Canary Islands and with estimates for plate motion of 2–8 mm/yr [12–14]. The presence of multiple cycles of volcanism on the older islands in the chain and the overall low productivity of the Canary hotspot suggests an origin involving an intermittent plume, or blobs, rather than a continuous plume [4,5].

The ~15 Myr subaerial volcanic history of Gran Canaria can be divided into two major cycles of volcanism (Fig. 2): the Miocene or shield cycle (< 15–9 Ma)—similar to the Hawaiian preshield,

shield and postshield stages—and the Pliocene or first rejuvenated cycle (5.5–1.7 Ma)—similar to the Hawaiian rejuvenated stage [4,5,9]. Quaternary (1.3–0 Ma) volcanism on Gran Canaria may represent the initiation of a second rejuvenated cycle. Cycles can be further subdivided into as many as four stages (see Fig. 2) [4,5]. A submarine Miocene stage 1, containing highly undersaturated volcanics, is inferred from the neighboring island of Fuerteventura (Fig. 1), where the earliest volcanics, which are intercalated with continental rise sediments, are subaerially exposed [11]. The oldest subaerial Miocene volcanics on Gran Canaria (Guigui Formation, > ca. 14.3 Ma) belong to the end of stage 2 and consist of picrites and tholeiites (Figs. 2 and 3). Miocene stage 3 volcanics (Hogarzales and Mogan Formations, ca. 14.3–13.5 Ma) become progressively more differentiated upsection and range from tholeiites and alkali basalts to trachytes and peralkaline rhyolites. Miocene stage 4 volcanics and intrusives (Fataga and Tejeda Formations, ca. 13–9 Ma) are the most SiO₂ undersaturated, consisting of trachyphonolites, nepheline syenites and rare nephelinites. Eruption rate and magma production rates (i.e., eruption rate corrected for volume loss due to crystal fractionation) were at a maximum during stage 2 and decreased throughout stage 3 (Fig. 2) [4]. There was a mild resurgence in both rates at the beginning of stage 4, followed by a continual decrease until volcanism ceased. During the Miocene, volcanism was highly centralized, with most magmas probably passing through a common plumbing network enroute to the surface.

The Pliocene cycle began after a > 3 Myr hiatus in volcanism (Fig. 2). Pliocene stage 1 volcanics (El Tablero Formation, ca. 5.3–4.8 Ma) consist of highly SiO₂-undersaturated basalts, including nephelinites, basanites and rare tephrites. During Pliocene stage 2 (lower Roque Nublo Group, ca. 4.7–4.0 Ma), only basalts were erupted, which became more SiO₂-saturated, from basanites to alkali basalts to tholeiites, with decreasing age. Pliocene stage 3 (upper Roque Nublo Formation, ca. 3.9–3.4 Ma) contains complete suites of alkali basalts through trachytes and basanites through phonolites, with the latter suite becoming more prevalent higher in the section. Eruption and magma production rates increased systematically with decreasing age during stages 1 and 2 and

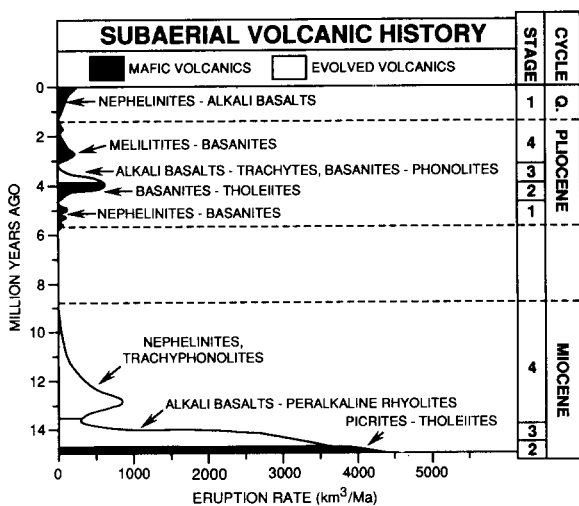


Fig. 2. Eruption rate versus age for the three cycles—Miocene (shield), Pliocene (first rejuvenated) and Quaternary (second rejuvenated?)—of subaerial volcanism on Gran Canaria [4]. Stippled pattern denotes predominantly mafic ($Mg\# > 62$) volcanism; whereas areas with no pattern denote periods of predominantly evolved ($Mg\# < 62$) volcanism. The Miocene cycle makes up ~80% of the subaerial volume, the Pliocene cycle ~18% and the Quaternary cycle ~2%.

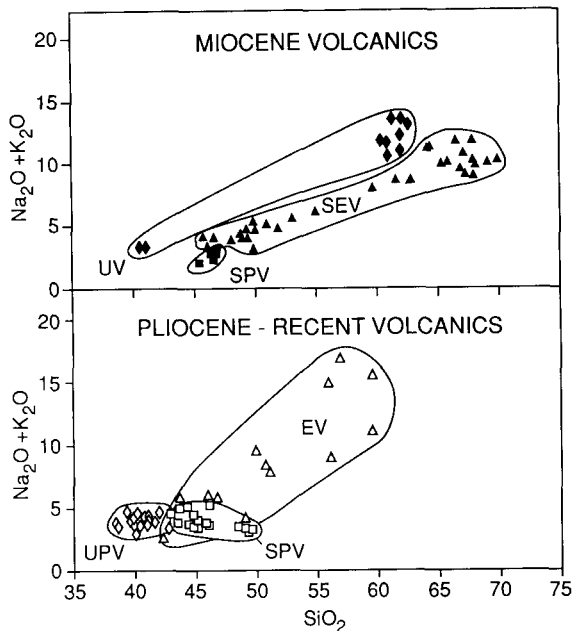


Fig. 3. Plot of SiO_2 versus the alkalis for the Miocene and Pliocene–Recent volcanics on Gran Canaria (only samples for which isotope data is available from this study and Cousens et al. [6] are included). The Miocene volcanics have been divided into three groups based on age and chemical compositions: (1) undersaturated volcanics (UV), which consist of nephelinites and trachyphonolites = stage 4; (2) saturated primitive volcanics (SPV), which have $\text{SiO}_2 > 43$ and magnesium number ($\text{Mg}\#$) > 62 , and include picrites and tholeiites = stage 2; and (3) saturated evolved volcanics (SEV), which have $\text{Mg}\# \leq 62$ and range from tholeiites to peralkaline rhyolites = stage 3. The Pliocene–Recent volcanics have also been divided into three groups: (1) undersaturated primitive volcanics (UPV), which have $\text{SiO}_2 < 43$ and $\text{Mg}\# > 62$, and range from basanites to melilitites = primarily stages 1 and 4; (2) saturated primitive volcanics (SPV), which have $\text{SiO}_2 \geq 43$ and $\text{Mg}\# > 62$, and range from basanites to tholeiites = primarily stage 2; and (3) evolved volcanics (EV), which have $\text{Mg}\# \leq 62$ and range from alkali basalts through trachytes and basanites through phonolites = primarily stage 3. The Miocene and Pliocene–Recent UV and UPV groups are collectively referred to as the most undersaturated groups, and the SEV and EV as the evolved groups. XRF data is from Cousens et al. [6], Hoernle and Schmincke [4] and references therein.

then decreased during stage 3 (Fig. 2) [15]. Following a possible brief hiatus in volcanism, there was a resurgence in volcanism, during which only highly undersaturated basalts were erupted. These Pliocene stage 4 basalts (Los Llanos and Los Pechos Formations, ca. 3.2–1.7 Ma) range in composition from basanite to melilitite. During stage 4, both SiO_2 -saturation and eruption rate in-

creased initially and then decreased. The oldest Quaternary basalts that have been dated are nephelinites, whereas the most recent Quaternary eruptives are predominantly basanites, with rare tephriphonolites and phonolites. In contrast to Pliocene stage 1 and 4 and Quaternary stage 1 volcanics, which were erupted from vents scattered across the whole island, most of the Pliocene stage 2 and 3 volcanics originated from a central eruption complex, located within the Miocene caldera (Fig. 1).

3. Analytical methods

Sample preparation and procedures for the isotopic analyses presented in Table 1 are the same as those outlined in Hoernle and Tilton [16]. Based on replicate analyses of sample material, the two sigma reproducibility is estimated to be better than ± 0.000025 for Sr, ± 0.000020 for Nd, and $\pm 0.05\%$ per amu for Pb isotope ratios. Comparison of the isotopic composition of leached and unleached sample material illustrates that acid washing does not significantly affect the Nd and Pb isotope ratios but may slightly lower the $^{87}\text{Sr}/^{86}\text{Sr}$ ratio. A table containing unleached isotope data and replicate analyses for Gran Canaria samples is available from the first author upon request. A more detailed discussion of the effects of acid washing, and of the reproducibility of isotopic and trace element data is presented in Hoernle and Tilton [16]. Isotope ratios were measured on a multiple collector Finnigan MAT 261 mass spectrometer operating in static mode. For consistency, the Pb, Sr and Nd analyses were normalized to the same values as those used in the earlier study on the Mogán and lower Fataga ignimbrites from Gran Canaria also performed at UCSB [6].

4. Results and observations

The Miocene and the Pliocene–Recent volcanics form distinct, elongate fields on isotope correlation diagrams (Figs. 4–7). In the Sr–Nd, Pb–Sr, Delta 208/204 Pb–Sr and Pb–Nd diagrams, the Miocene and Pliocene–Recent fields form different trends. For example, the Miocene volcanics form trends with zero slope in the Sr–Nd and Pb–Nd diagrams, whereas the Pliocene–Re-

TABLE 1
Isotope data from Gran Canaria volcanics in order of increasing age and sediments from DSDP site 397

Sample number	Rock type	Rock group	Age (Ma)	SiO ₂ (wt%)	Mg#	Rb (ppm)	Sr (ppm)	⁸⁷ Sr/ ⁸⁶ Sr _{in.}	Sm (ppm)	Nd (ppm)	¹⁴³ Nd/ ¹⁴⁴ Nd _{in.}	Epsilon Nd	Pb (ppm)	U (ppm)	Th (ppm)	²⁰⁶ Pb/ ²⁰⁴ Pb _{in.}	²⁰⁷ Pb/ ²⁰⁴ Pb _{in.}	²⁰⁸ Pb/ ²⁰⁴ Pb _{in.}	
<i>Quaternary</i>																			
Q1499	basanite	UPV	0.0	42.7	71.0	29.91	880.2	0.703172(16)	10.68	56.26	0.512909(5)	5.29	3.04	1.30	4.40	19.542	15.592	39.382	
Q1433	basanite	SPV	0.0	43.6	67.4	29.38	934.1	0.703158(21)	11.11	56.05	0.512930(8)	5.70	3.28	1.25	4.82	19.473	15.583	39.333	
Q1414	basanite	UPV	0.2	42.8	65.7	37.93	1165	0.703164(14)	12.17	65.59	0.512907(7)	5.24	3.32	1.49	5.66	19.507	15.587	39.385	
Q1714A	basanite	EV	0.5	42.2	52.8	* 11	* 2832	0.703136(16)			0.512866(8)	4.45				19.479	15.579	39.334	
Q1438	tephrite	EV	0.9	43.7	61.0	* 38	* 1538	0.703250(14)	* 15.73	* 91.17	0.512872(9)	4.56	5.48	2.60	10.41	19.490	15.566	39.338	
QC21	nephelinite	UPV	1.3	40.1	71.8	* 35	* 1439	0.703118(17)	* 14.45	* 84.3	0.512953(6)	6.14		* 9.5	19.485	15.584	39.247		
<i>Pliocene</i>																			
LLC22	melilitite	UPV	1.7	38.3	76.1	* 14	* 1333	0.703104(12)	* 15.5	* 88	0.512957(6)	6.22	4.97	2.42	10.14	19.567	15.605	39.518	
LL1415	melilitite	UPV	1.8	39.3	72.5	32.70	1351	0.703117(16)	18.78	104.53	0.512930(6)	5.69	4.58	2.52	10.13	19.329	15.568	39.126	
LLC9	melilitite	UPV	1.9	38.5	69.4	* 12	* 1787	0.703126(16)	* 18.8	* 106	0.512931(5)	5.71	2.24	2.24	10.26	19.531	15.589	39.390	
LL1410	hawaite	SPV	1.9	46.1	64.4	41.89	1203	0.703186(11)	12.59	66.75	0.512849(12)	4.11	5.63	* 1.9	7.06	19.159	15.558	39.061	
LL1142	nephelinite	UPV	2.4	39.7	68.9	* 41	* 1490	0.703189(17)	* 16.6	* 84.4	0.512898(3)	5.07	3.75	1.87	7.32	19.364	15.577	39.225	
LL1141	nephelinite	UPV	2.6	40.0	72.0	26.26	1604	0.703183(12)	17.73	100.01	0.512894(10)	5.00	3.34	2.49	9.72	19.502	15.583	39.382	
LLC16	nephelinite	UPV	2.9	40.7	72.3	* 30	* 1204	0.703066(13)	* 13.6	* 73	0.512967(6)	6.42	3.65	1.76	7.21	19.383	15.567	39.153	
LL1424	nephelinite	UPV	3.1	39.9	70.7	24.47	1478	0.703097(11)	17.04	93.01	0.512899(15)	5.09	2.71	2.10	7.68	19.478	15.582	39.307	
RNB122	phonolite	EV	3.4	56.0	28.7	* 143	* 2394	0.703290(12)	4.38	32.26	0.512779(7)	2.75	14.74	3.61	21.41	19.187	15.536	39.197	
RNC44	basanite	UPV	3.4	41.6	70.2	* 33	* 1061	0.703090(15)			0.512981(6)	6.69	28.93	13.06	40.32	19.174	15.526	39.175	
RNC1	phonolite	EV	3.4	56.9	10.6	231.1	139.7	0.703493(23)	1.83	15.92	0.512846(12)	4.07							
RNC1	anorthoclase					124.7	773.7	0.703295(15)											
RNC49	basanite	UPV	3.5	42.0	70.0	* 24	* 1358	0.703122(12)	* 11.4	* 59	0.512927(6)	5.64	4.78	1.35	5.39	19.361	15.562	39.207	
RNI179	hawaite	EV	3.5	46.7	50.7	* 73	* 1665	0.703173(16)	16.26	92.31	0.512827(3)	3.68	5.01	2.22	9.54	19.076	15.519	38.978	
RNI143	phonotephrite	EV	3.5	49.9	47.8	101.1	2148	0.703272(15)	16.38	98.16	0.512846(12)	4.05	9.20	4.58	17.23	19.165	15.541	39.185	
RNC25	phonolite	EV	3.5	59.6	12.2	187.5	56.92	0.703606(16)	2.57	28.28	0.512789(7)	2.94	17.85	8.03	28.58	19.216	15.530	39.184	
RNC25	anorthoclase					71.28	610.2	0.703199(11)											
RNB105	basanite	SPV	3.5	44.7	64.1	* 48	* 911	0.703156(14)	* 10.5	* 53.4	0.512879(6)	4.71	2.42	1.04	4.82	19.177	15.529	39.002	
RNI130	basanite	UPV	3.6	42.7	67.5	19.39	940.6	0.703079(12)	12.47	60.67	0.512901(7)	5.13	2.70	* 1.06	4.36	19.243	15.551	39.035	
RNB44	phonotephrite	EV	3.6	50.7	47.1	42.01	1835	0.703324(17)	16.13	97.53	0.512761(7)	2.39	7.07	3.03	12.71	19.165	15.534	39.241	
RNB36	mugearite	EV	3.6	51.1	47.9	46.12	1739	0.703273(15)	14.79	87.98	0.512755(6)	2.29	6.98	2.96	11.30	18.979	15.511	38.984	
RNI74	trachyte	EV	3.6	59.5	31.0	110.1	2189	0.703293(15)	6.05	50.91	0.512761(9)	2.40	12.28	3.97	17.59	19.133	15.542	39.269	
RNB31	benmoreite	EV	3.7	56.2	43.9	62.06	1753	0.703232(13)	12.08	76.46	0.512777(5)	2.70	8.99	2.57	16.06	19.115	15.530	39.103	
RNI86	alkali																		
RNB3.3	basalt	SPV	3.7	46.0	62.8	* 31	* 825	0.703114(13)	11.40	54.63	0.512879(7)	4.70	1.95	0.84	3.53	19.174	15.537	39.006	
RNB3.3	tholeiite	EV	3.9	49.6	61.7	15.63	529.0	0.703191(11)	7.48	31.07	0.512883(9)	4.78	1.48	0.42	1.86	18.994	15.588	38.992	

RN63.2	tholeiite	SPV	3.9	48.9	63.1	* 13	* 550	0.703160(15)	0.512886(4)	4.84	19.019	15.578	39.004	
RN63.1	tholeiite	EV	3.9	49.4	51.6	7.44	579.3	0.703188(14)	0.512890(7)	4.92	2.05	19.007	15.559	38.974
RNB14	tholeiite	SPV	4.0	48.8	65.1	11.00	536.7	0.703204(16)	0.512879(7)	4.71	1.39	19.008	15.569	38.944
RN60	tholeiite	SPV	4.0	48.4	63.3	9.55	564.8	0.703147(6)	0.512879(6)	4.71	1.75	19.036	15.571	38.966
RN951	basanite	SPV	4.1	44.2	65.2	35	* 1262	0.703191(15)	0.512857(8)	4.28	3.33	19.219	15.570	39.228
RN1258	basanite	SPV	4.1	44.8	65.2	* 34	* 1061	0.703154(17)	0.512865(5)	4.43	3.51	19.124	15.541	39.074
RN53	alkali													
basalt		SPV	4.1	45.7	65.5	22.83	871.8	0.703186(24)	0.512872(6)	4.56	2.87	19.008	15.545	38.955
RNB125	basanite	SPV	4.2	43.4	64.1	* 46	* 1076	0.703126(10)	0.512847(10)	4.08	3.27	19.181	15.540	39.070
RN54	basanite	EV	4.2	45.0	60.8	* 31	* 1011	0.703094(12)	0.512916(7)	5.42	2.36	19.190	15.553	39.078
RNB60	basanite	SPV	4.3	44.2	68.0	* 42	* 1106	0.703218(14)	0.512831(7)	3.76	0.74	19.149	15.552	38.994
RN1249	alkali													
basalt		SPV	4.4	45.0	65.5	* 23	* 1328	0.703165(15)	0.512828(6)	3.70	4.20	19.030	15.521	39.024
RN104	basanite	EV	4.4	44.0	61.4	* 25	* 1144	0.703226(13)	0.512818(5)	3.51	1.27	19.149	15.532	38.994
RN99.2	basanite	SPV	4.5	44.4	66.7	* 30	* 1002	0.703112(16)	0.512913(6)	5.37	2.49	19.149	15.532	38.994
RN94	alkali													
basalt		SPV	4.5	45.1	69.5	* 32	* 868	0.703082(13)	0.512959(6)	6.27	2.57	19.361	15.549	39.101
RN95	basanite	SPV	4.6	44.6	69.9	* 43	* 1147	0.703095(14)	0.512934(6)	5.78	3.51	19.494	15.570	39.276
RN677	basanite	SPV	4.7	43.1	64.4	* 24	* 1234	0.703101(15)	0.512898(5)	5.07	3.34	19.209	15.573	39.129
ETB45	nephelinite	UPV	5.0	40.0	71.0	27.25	1064	0.703089(18)	0.512888(6)	4.88	3.09	19.475	15.572	39.226
ET88	nephelinite	UPV	5.0	40.3	70.5	6.66	1348	0.703106(16)	0.512907(6)	5.25	2.66	19.449	15.573	39.216
ETB47	nephelinite	UPV	5.0	41.0	68.2	25.90	939.9	0.703078(16)	0.512898(8)	5.07	2.22	19.443	15.571	39.185
ET108	tephrite	EV	5.2	45.9	52.4	47.48	1579	0.703235(14)	0.512771(11)	2.60	5.31	18.760	15.501	38.866
ET106	basanite	UPV	5.3	41.0	66.3	* 35	* 857	0.703092(16)	0.512920(4)	5.49	2.49	19.359	15.575	39.170
ET878	basanite	UPV	5.3	41.0	65.7	28.73	921.6	0.703121(12)	0.512900(10)	5.11	1.96	19.312	15.593	39.154
Miocene														
Tl376	trachyte	UV	11.4	61.3	17.3	135.0	3.67	0.703075(15)	0.512887(7)	4.85	13.60	19.888	15.585	39.603
Tl374	trachyte	UV	11.4	62.6	16.0	119.1	4.44	0.703075(39)	0.512887(5)	4.86	13.21	19.921	15.631	39.725
TC43	phonolite	UV	11.6	62.2	18.8	118.0	7.19	0.703020(25)	0.512893(6)	4.70	12.02	20.014	15.627	39.783
TC43	felsic phases		11.6			163.6	2.47	0.703020(11)						
F253872	nephelinite	UV	11.8	40.5	53.4	19.51	* 2872	0.703079(6)	0.512901(3)	5.13	2.08	19.885	15.609	39.618
H1389	tholeiite	SEV	14.3	51.7	48.6	28.80	695.4	0.703350(17)	0.512906(9)	5.23	2.50	19.516	15.601	39.252
H1390	tholeiite	SEV	14.3	49.3	49.2	21.79	636.7	0.703341(14)	0.512899(9)	5.09	2.41	19.536	15.602	39.281
H1384	mugearite	SEV	14.3	52.9	44.2	36.57	774.8	0.703337(19)	0.512895(12)	5.02	3.47	19.577	15.591	39.283
H1383	tholeiite	SEV	14.3	49.9	44.4	39.07	598.2	0.703319(17)	0.512911(7)	5.33	3.50	19.562	15.596	39.292
H1382	tholeiite	SEV	14.3	48.9	45.5	23.73	588.3	0.703319(9)	0.512913(7)	5.36	2.50	19.512	15.592	39.218
G1392	tholeiite	SEV	14.4	49.8	58.5	15.76	539.3	0.703462(16)	0.512890(8)	4.91	2.37	19.366	15.606	39.108
G1378	tholeiite	SPV	14.4	46.7	65.9	19.93	513.2	0.703193(20)	0.512906(9)	5.23	2.14	19.636	15.627	39.409
G1379	tholeiite	SPV	14.4	46.4	69.2	21.62	533.1	0.703196(18)	0.512895(7)	5.02	2.19	19.647	15.611	39.376
G1377	tholeiite	SPV	14.5	46.6	74.3	7.63	323.4	0.703280(19)	0.512908(7)	5.27	1.50	19.572	15.599	39.257
G1265	tholeiite	SPV	14.5	46.9	70.4	22.88	358.1	0.703267(17)	0.512898(14)	5.07	2.09	19.549	15.621	39.307
G1262	tholeiite	SPV	14.5	45.4	78.5	14.80	237.9	0.703260(16)	0.512915(5)	5.41	1.30	19.527	15.619	39.288

TABLE 1 (continued)

Sample number	Rock type	Rock group	Age (Ma)	SiO ₂ (wt%)	Mg#	Rb (ppm)	Sr (ppm)	⁸⁷ Sr/ ⁸⁶ Sr _{in.}	Sm (ppm)	Nd (ppm)	¹⁴³ Nd/ ¹⁴⁴ Nd _{in.}	Epsilon Nd	Pb (ppm)	U (ppm)	Th (ppm)	²⁰⁶ Pb/ ²⁰⁴ Pb _{in.}	²⁰⁷ Pb/ ²⁰⁴ Pb _{in.}	²⁰⁸ Pb/ ²⁰⁴ Pb _{in.}	
<i>DSDP</i>																			
397-60-4	sediments	Tmu				165.8	397.1	0.710291(12)	5.42	28.74	0.511958(7)	-13.26	25.02	2.54	10.81	19.008	15.744	39.187	
397-101-1	sediments	Tmm				39.23	1240	0.723619(13)	2.60	14.10	0.512065(7)	-11.18	6.01	2.00	3.25	18.836	15.696	39.057	
397-30-1	sediments	Tml				69.38	135.7	0.709362(23)	3.68	19.86	0.511646(12)	-19.35	11.34	1.83	6.02	18.936	15.724	38.973	
397-40-2	sediments	Kh				45.99	1127	0.709363(16)	2.76	14.67	0.512038(6)	-11.70	6.08	1.65	3.45	18.605	15.685	38.947	
397-49-1	sediments	Kh				44.16	1203	0.709288(25)	3.03	16.49	0.512062(8)	-11.24	5.71	1.35	3.41	18.640	15.680	38.925	

Capital letters in front of sample numbers stand for the following formations: Q = Quaternary, LL = Los Llanos, RN = Roque Nublo, ET = El Tablero, T = Tejada, F = Fataga, H = Hogarales, and G = Guigui. The sources of most ages are reported in [4]. Ages for samples T1374, T1376 and TC43 were determined from the Sr isotope data, using the average initial ⁸⁷Sr/⁸⁶Sr ratio (0.703075) of Fataga and Tejada samples [this study and 6] for samples T1374 and T1376. Mg# { = Mg/(Mg + Fe⁺²) with Fe⁺³/(Fe⁺³ + Fe⁺²) = 0.2} and SiO₂ are from X-ray fluorescence data, recalculated on an anhydrous basis, reported in Schmincke [9,42] and Hoernle and Schmincke [4]. Trace element concentrations were determined by isotope dilution, except those preceded by an asterisk which were determined by XRF (Rb, Sr) or INAA (Sm, Nd, U, Th) [4]. The precision of all concentrations determined by isotope dilution is better than 1%. For determination of isotope ratios, a separate split of the same powder as used for the trace element analyses was acid washed for 45 min with a mixture of 50°C 6 N HCl and 7 N HNO₃, except for samples T1374, T1376, TC43 and the DSDP sediment samples. Felsic mineral separates were washed for 15 min with 2 N HCl. All isotope ratios are age corrected, except for the DSDP samples and the samples for which there is insufficient parent-daughter data. Errors refer to the least significant digits and are 2 sigma mean within-run precision. The ⁸⁷Sr/⁸⁶Sr ratio was normalized within-run to ⁸⁶Sr/⁸⁸Sr = 0.1194, and then adjusted to a ⁸⁷Sr/⁸⁶Sr value of 0.710250 for NBS 987. The ¹⁴³Nd/¹⁴⁴Nd ratio was normalized within-run to ¹⁴⁶Nd/¹⁴⁴Nd = 0.721900, and then adjusted to a ¹⁴³Nd/¹⁴⁴Nd value of 0.511850 for the La Jolla standard. Pb isotope analyses were corrected to NBS981 [43] for fractionation. An average of twelve measurements of NBS981 yielded: ²⁰⁶Pb/²⁰⁴Pb = 16.904(7), ²⁰⁷Pb/²⁰⁴Pb = 15.447(8) and ²⁰⁸Pb/²⁰⁴Pb = 36.560(21). Blanks for Sr, Nd and Pb were ≤ 0.3 nanograms and thus are negligible. ε_{Nd} was calculated using the initial ¹⁴³Nd/¹⁴⁴Nd ratio except for the sediment samples. ε_{Nd} = [(¹⁴³Nd/¹⁴⁴Nd)_{sample} / (¹⁴³Nd/¹⁴⁴Nd)_{bulk earth} - 1] × 10⁴. Bulk Earth = 0.512638; ¹⁴⁷Sm/¹⁴⁴Nd = 0.1966.

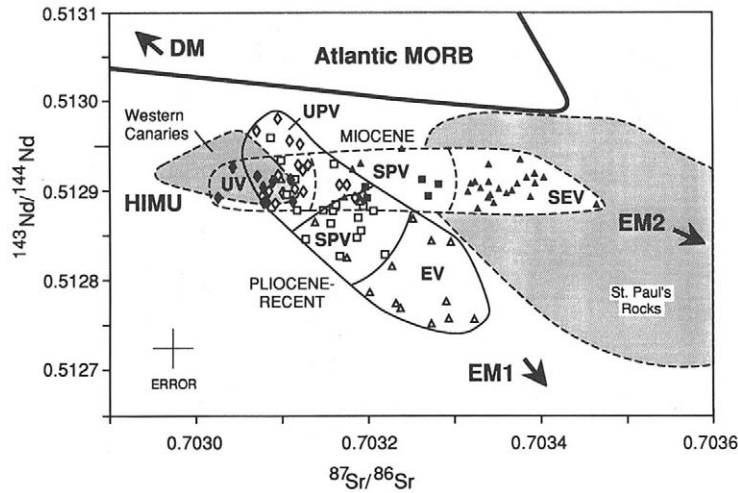


Fig. 4. Sr–Nd isotope correlation diagram for Gran Canaria volcanics. The fields for the Miocene (solid symbols) and Pliocene–Recent (open symbols) volcanics form different trends. The Miocene volcanics trend from a HIMU-like to an EM2-like composition. The Pliocene–Recent volcanics trend from an intermediate (HIMU + DM + EM) composition towards EM1. The most undersaturated volcanics (UV, UPV; diamonds) from the two groups overlap with the field for the western Canary Islands of La Palma and Hierro [Hoernle et al., manuscript in preparation], which primarily reflects interaction between the Canary Plume (HIMU-like) and the asthenosphere (DM + EM). The saturated primitive volcanics (SPV; squares) and the evolved volcanics (SEV, EV; triangles) extend towards more enriched compositions, with the evolved volcanics having the most enriched compositions. The trend towards more enriched compositions probably results from lithospheric contamination, with the lower lithosphere beneath Gran Canaria having an EM2-like and the upper lithosphere an EM1-like composition. Also shown is the field for St. Paul’s Rocks, a piece of mantle peridotite subaerially exposed along a mid-Atlantic-ridge transform fault [19]. The figure also contains Miocene data from Cousens et al. [6]. The mantle components are from Zindler and Hart [1] and the field for Atlantic MORB is from Ito et al. [23].

cent volcanics form trends with a negative slope in the Sr–Nd diagram and a positive slope in the Pb–Nd diagram (Figs. 4 and 7). Although the

Miocene samples cover a time period > 3 Myr, $^{143}\text{Nd}/^{144}\text{Nd}$ is surprisingly constant at 0.512900 ± 0.000018 (2 sigma, $N = 15$, this study) and 0.512913 ± 0.000030 (2 sigma, $N = 30$, [6]), within the analytical precision for each study. The average $^{143}\text{Nd}/^{144}\text{Nd}$ ratio for all the analyzed Miocene samples (0.512910 ± 0.000030 , 2 sigma, $N = 45$) is also indistinguishable from the average value for the western islands of La Palma and Hierro (0.512921 ± 0.000041 , 2 sigma, $N = 17$

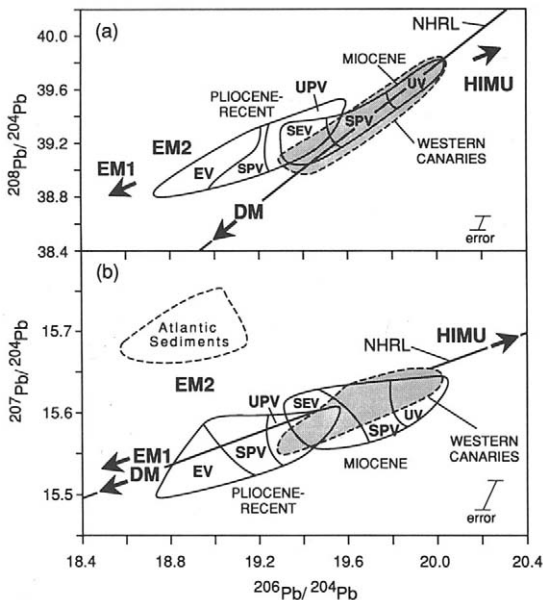


Fig. 5. Pb–Pb isotope correlation diagrams for Gran Canaria volcanics. The Pliocene–Recent group has less radiogenic Pb isotopes than the Miocene group. Both groups form trends which have nearly horizontal to positive slopes. Within a group, the most undersaturated volcanics have the most radiogenic Pb and the evolved volcanics the least radiogenic. On the $^{207}\text{Pb}/^{204}\text{Pb}$ diagram both groups fall on the northern hemisphere reference line (NHRL) [17]. Neither group trends towards the field for Atlantic sediments, which contains data from this study and Sun [18]. On the $^{208}\text{Pb}/^{204}\text{Pb}$ diagram, some of the Miocene evolved volcanics and the Pliocene–Recent volcanics fall above the NHRL. For additional information and references see caption to Fig. 4.

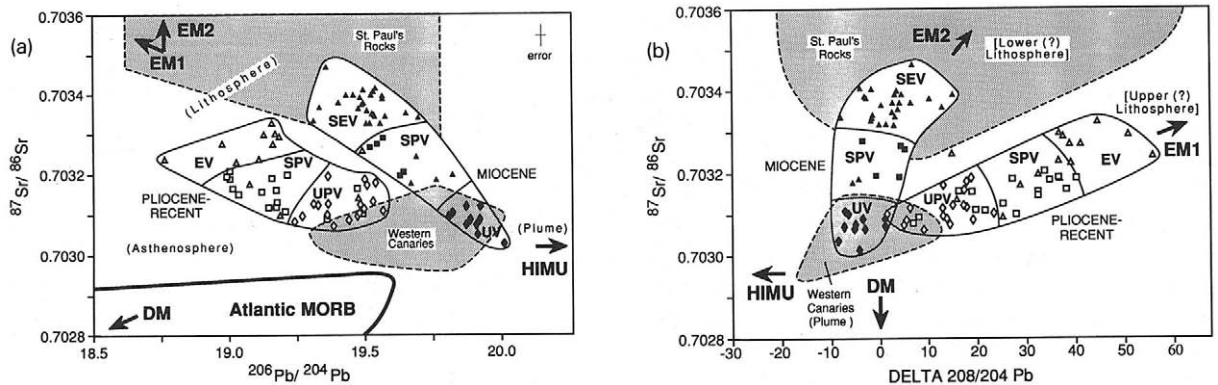


Fig. 6. Pb–Sr isotope correlation diagrams for Gran Canaria volcanics: (a) $^{206}\text{Pb}/^{204}\text{Pb}$ versus $^{87}\text{Sr}/^{86}\text{Sr}$, and (b) Delta 208/204 Pb versus $^{87}\text{Sr}/^{86}\text{Sr}$. See caption to Fig. 4 for additional information and references.

[Hoernle et al., in prep.]). As illustrated in Fig. 6, $^{87}\text{Sr}/^{86}\text{Sr}$ correlates negatively with the Pb isotope ratios and positively with Delta 208/204 Pb (the deviation from the Northern Hemisphere Reference Line (NHRL) [17]). The range in Pb isotopes for Gran Canaria ($^{206}\text{Pb}/^{204}\text{Pb} = 18.76\text{--}20.01$) covers the entire range reported for the other Canary Islands [18]. The Pliocene–Recent volcanics have less radiogenic Pb isotopes than the Miocene volcanics (Fig. 5). In the $^{206}\text{Pb}/^{204}\text{Pb}$ versus $^{207}\text{Pb}/^{204}\text{Pb}$ diagram, both fields have slightly positive slopes and intersect the NHRL. Neither field trends towards Cretaceous–Recent Atlantic sediments. In the $^{206}\text{Pb}/^{204}\text{Pb}$ versus

$^{208}\text{Pb}/^{204}\text{Pb}$ diagram, the trends for both groups also have positive slopes. The Miocene volcanics with the most radiogenic ^{206}Pb fall on the NHRL in this diagram; some of the Miocene samples with the least radiogenic ^{206}Pb and the Pliocene–Recent samples, however, fall above the NHRL and thus have Delta 208/204 Pb > 0 (Fig. 6b).

Based on their major element compositions and stage of eruption, both the Miocene and Pliocene–Recent volcanics can be subdivided into three groups (Fig. 3), which also have different isotopic compositions. The Pliocene–Recent undersaturated primitive volcanics (UPV) have magnesium numbers ($\text{Mg}\#$) ≥ 66 and $\text{SiO}_2 < 43$

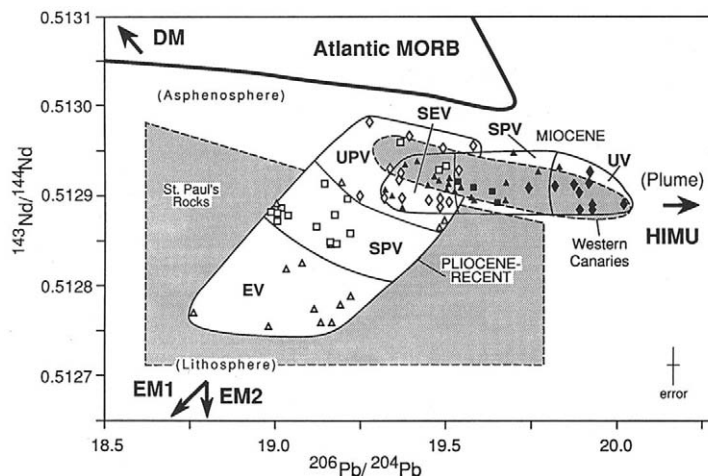


Fig. 7. Pb–Nd isotope correlation diagram for Gran Canaria volcanics. See caption to Fig. 4 for additional information and references.

weight percent, and range from basanites to melilitites; the Miocene undersaturated volcanics (UV) are nephelinites and trachyphonolites. The UPV were erupted during stages 1 and 4 of the Pliocene and Quaternary Cycles, and the UV during Miocene stage 4 (Fig. 2). As mentioned previously, Miocene stage 1 volcanics are not exposed on Gran Canaria. The saturated primitive volcanics (SPV) have $Mg\# > 62$ and $SiO_2 \geq 43$ weight percent and range from basanites to tholeiites and picrites. These volcanics were primarily erupted during stage 2 of each cycle. The Miocene saturated evolved volcanics (SEV) and the Pliocene–Recent evolved volcanics (EV) have $Mg\# < 62$ and were erupted primarily during stage 3 of each cycle.

In all isotope correlation diagrams (Figs. 4–7), the most SiO_2 -undersaturated volcanics from each cycle (UV, UPV) have the most restricted compositional range and fall at the end of the field for each cycle that overlaps the field for the western Canary Islands. For each cycle, these volcanics have the least radiogenic $^{87}Sr/^{86}Sr$, the most radiogenic $^{206}Pb/^{204}Pb$ and $^{208}Pb/^{204}Pb$, and lowest Delta 208/204 Pb values. The UPV also have the most radiogenic $^{143}Nd/^{144}Nd$ ratios of the Pliocene–Recent volcanics. The Miocene SPV fall in the middle of the Miocene field, and the Pliocene–Recent SPV are concentrated in the middle of the Pliocene–Recent field but also overlap the UPV. The evolved (SEV, EV) groups cover most of the field for a cycle but are concentrated on the opposite ends of the fields from the most undersaturated volcanics. The evolved groups have the most radiogenic Sr and the least radiogenic Pb isotopic compositions, and the highest Delta 208/204 Pb values. The EV also have the least radiogenic Nd isotopic compositions of the Pliocene–Recent volcanics. In Figs. 4, 6 and 7, the Miocene volcanics trend towards the field for St. Paul's Rocks [19], with the SEV overlapping the field. St. Paul's Rocks are a piece of mantle peridotite that is subaerially exposed along the St. Paul Fracture Zone on the Mid Atlantic Ridge.

Sr, Nd and Pb isotopes show systematic and similar variations with $Mg\#$ for the Pliocene volcanics (Fig. 8). With decreasing $Mg\#$, $^{87}Sr/^{86}Sr$ increases and the $^{143}Nd/^{144}Nd$ and Pb isotope ratios decrease until $Mg\#$ is ~ 50 ; below this value all ratios remain roughly constant. $Mg\# =$

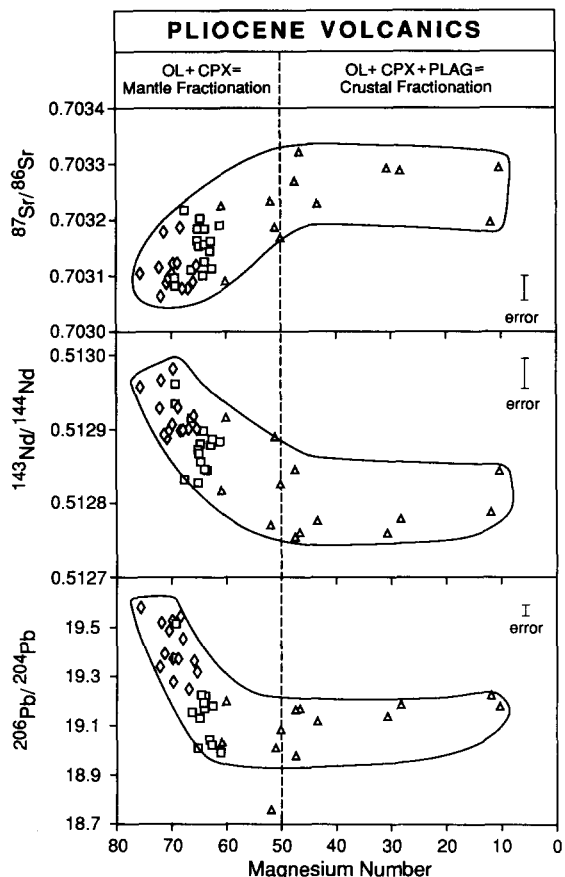


Fig. 8. Plots of magnesium number ($Mg\#$) versus Sr, Nd and Pb isotope ratios for the Pliocene volcanics illustrate assimilation during crystal fractionation. With decreasing $Mg\#$, the $^{87}Sr/^{86}Sr$ ratio increases and the $^{143}Nd/^{144}Nd$ and $^{206}Pb/^{204}Pb$ ratios decrease and then remain constant. The change in slope of the trends at $Mg\# = 50$ corresponds with the crystallization of plagioclase. The presence of plagioclase on the liquidus may mark the transition from mantle to crustal levels of cooling and fractionation [4].

50 also divides rocks which only have olivine and clinopyroxene on the liquidus ($Mg\# > 50$) from rocks which also have plagioclase on the liquidus ($Mg\# < 50$). Although not as abundant as in the hawaiite to trachyte suite, plagioclase is present as a phenocryst phase in the tephrite to phonolite suite and is required in the mass balance calculations to link rocks in this suite by fractional crystallization [15]. There is no simple correlation between $Mg\#$ and isotopic composition for the Miocene volcanics.

The mafic and evolved volcanics from the nearby Cape Verde Islands exhibit similar isotopic

variations to the Pliocene–Recent volcanics on Gran Canaria. Although the isotopic compositions of the evolved volcanics from the Cape Verde Islands overlap those of the mafic lavas (based on data from Gerlach et al. [20]), the evolved volcanics tend to lie at the end of the mafic field which has the most radiogenic Sr and the least radiogenic Nd and Pb isotopes. Considering only volcanics from the same formation, such as from the Pico de Antonio Formation (< 11 , > 5 Ma) on São Tiago, the isotopic distinction between mafic and evolved volcanics is quite impressive (Fig. 9). The mafic lavas—basanites and nephelinites—are completely distinct in all isotopic ratios from the associated evolved volcanics—tephrites and phonolites.

Figure 10 illustrates that stages 2–4 of the Miocene and Pliocene cycles and possibly stage 1

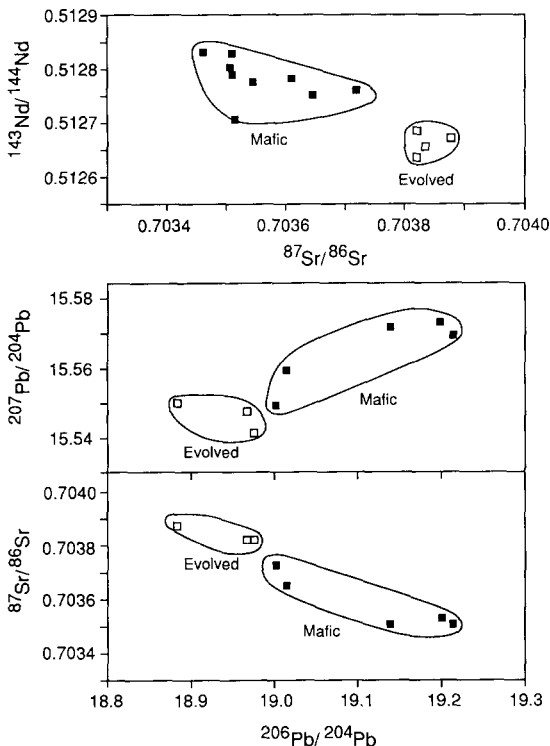


Fig. 9. The mafic lavas (solid squares) and the evolved volcanics (open squares) from the Pico de Antonio Formation on São Tiago, Cape Verde Islands [20] form distinct fields on isotope correlation diagrams. Similar to the Pliocene volcanics on Gran Canaria, the mafic lavas—basanites and nephelinites—have more radiogenic Nd and Pb and less radiogenic Sr isotopes, whereas the evolved volcanics—tephrites and phonolites—have more radiogenic Sr and less radiogenic Nd and Pb isotopes.

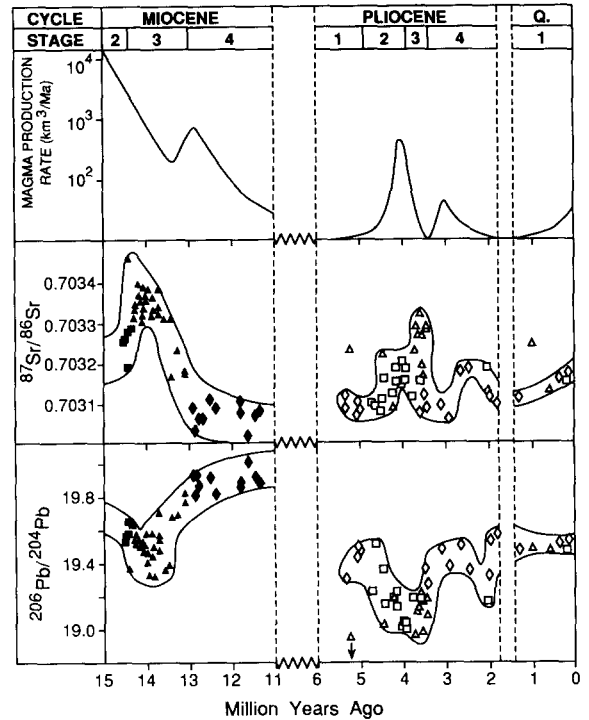


Fig. 10. Age in million years ago versus the magma production rate (eruption rate with a correction for volume loss due to crystal fractionation [4,15]), $^{87}\text{Sr}/^{86}\text{Sr}$ and $^{206}\text{Pb}/^{204}\text{Pb}$. When the same stages of cycles are compared, the isotopic variations with age for each cycle are similar, indicating that the different cycles have similar temporal isotopic evolutions. The peaks (positive for Sr and negative for Pb) in isotopic composition, which occur during stage 3 and possibly late stage 4 in the Pliocene Cycle, do not correlate with the peaks in magma production rate, which occur during stage 2 and early stage 4. The highest Sr and the lowest Pb isotope ratios are primarily present in volcanics erupted during declining magma production rate. Symbols and data sources are the same as in Fig. 4.

of the Pliocene and the Quaternary Cycles had similar temporal evolutions in Sr and Pb isotopic composition. Although the isotope ratios covary with the magma production rate, the peaks in isotopic composition for each cycle—i.e., highest $^{87}\text{Sr}/^{86}\text{Sr}$, lowest $^{206}\text{Pb}/^{204}\text{Pb}$ and lowest $^{143}\text{Nd}/^{144}\text{Nd}$ for the Pliocene Cycle (not shown)—do not correspond to the peaks in magma production rates. Instead, the peaks in isotopic composition occurred as the magma production rate decreased.

5. Discussion

Several factors favor mixing of four components to explain the variation in isotopic composi-

tion observed on Gran Canaria: (1) Both the Miocene and Pliocene–Recent volcanics form elongate trends on isotope correlation diagrams. (2) The isotopic composition for each group correlates with major element composition. (3) The most undersaturated volcanics from each group always fall on the end of a given trend that intersects the field for the western Canary Islands, while the evolved volcanics extend to the opposite end of each trend, and the primitive saturated volcanics are concentrated in the middle of both trends.

The four components responsible for the chemical compositions of the Gran Canaria magmas are best represented by: (1) the Miocene UV with $^{87}\text{Sr}/^{86}\text{Sr} \leq 0.7030$, $^{143}\text{Nd}/^{144}\text{Nd} = 0.51291$, $^{206}\text{Pb}/^{204}\text{Pb} \geq 20.0$ and $\Delta 208/204 \text{ Pb} = 0$; (2) the Pliocene–Recent UPV with $^{87}\text{Sr}/^{86}\text{Sr} \leq 0.7031$, $^{143}\text{Nd}/^{144}\text{Nd} \geq 0.51298$, $^{206}\text{Pb}/^{204}\text{Pb} \geq 19.6$ and $\Delta 208/204 \text{ Pb} = 0$; (3) the Miocene SEV with $^{87}\text{Sr}/^{86}\text{Sr} \geq 0.7035$, $^{143}\text{Nd}/^{144}\text{Nd} \leq 0.51291$, $^{206}\text{Pb}/^{204}\text{Pb} \leq 19.3$ and $\Delta 208/204 \text{ Pb} > 0$; and (4) the Pliocene EV with $^{87}\text{Sr}/^{86}\text{Sr} \geq 0.7033$, $^{143}\text{Nd}/^{144}\text{Nd} \leq 0.51275$, $^{206}\text{Pb}/^{204}\text{Pb} \leq 18.8$ and $\Delta 208/204 \text{ Pb} > 0$. In the following discussion, we use correlations of isotopic composition with major element composition, magma production rate and age, and comparisons to the isotopic composition of other volcanoes from the Canary Islands to constrain the location of these components in the crust and mantle beneath Gran Canaria.

5.1. Composition of the Canary Plume and asthenosphere (UV and UPV endmembers)

Several factors are consistent with the volcanics from the western Canary Islands having the most plume-like isotopic compositions. Based on the east to west age progression in the Canary Chain and in view of the abundant historic activity as recent as 1971 on La Palma, the center of the Canary Plume should presently be situated beneath the westernmost islands of Hierro and La Palma [9]. These islands are also the farthest from the African continental margin and thus are the least likely to be contaminated by continentally derived sediments or continental lithospheric mantle recycled during rifting. The most undersaturated volcanics (UV and UPV, endmembers 1

and 2 above) from each group on Gran Canaria fall within or overlap the field for the western Canary Islands, suggesting that these volcanics may have the most plume-like compositions of the volcanics on Gran Canaria. The field for the western Canary Islands trends from a HIMU-like composition towards a slightly enriched DM-like component similar to E-MORB, which may represent a mix of predominantly DM with minor amounts of EM material [Hoernle et al., manuscript in prep.]. Similar trends from HIMU-like to DM-like compositions are observed (1) in primitive Holocene basanites with increasing distance from the westernmost islands, and (2) between the Miocene UV and the Pliocene UPV. These trends are interpreted to reflect interaction of plume material or melts, having a HIMU-like composition, with primarily asthenospheric (\pm lithospheric) material or melts, having a DM-like composition [Hoernle et al., manuscript in prep., 16]. This interpretation implies that none of the subgroups on Gran Canaria directly reflect (i.e., neither the Miocene or Pliocene–Recent volcanics directly trend towards) the plume or asthenospheric composition, but instead represent mixtures of these reservoirs.

5.2. Composition of the lithosphere beneath Gran Canaria (SEV and EV endmembers)

5.2.1. Assimilation during fractional crystallization (AFC)

The major and trace element data, combined with the magma production rates, indicate that the saturated primitive volcanics (SPV) were derived by higher degrees of partial melting of an asthenospheric (presumably plume) source than the undersaturated primitive volcanics [4,5]. Therefore, the differences in isotopic composition between the undersaturated and saturated primitive volcanics might be related to the degree of partial melting of a heterogeneous plume (e.g. [21]). If this were the case, we would expect to find isotopic compositions similar to the SPV among the western Canary basalts, since the range in major element compositions of the primitive basalts from the western Canary Islands is similar to that observed on Gran Canaria. There is, however, not such overlap. Moreover, the variations in isotopic composition should correlate with the variations

in magma production rate (Fig. 10). There is considerable uncertainty in the absolute values of the magma production rate, but the general shapes of the curves are reasonably well constrained [3,9,10,15 and references therein]. Although the patterns in isotopic composition and magma production rate are similar in Fig. 10, the most extreme peaks (Gran Canaria endmembers 3 and 4 above) occur during declining magma production rates, when the volcanics have predominantly evolved compositions (stage 3).

The evolved volcanics from each age group (SEV, EV) can be derived from primitive basalts from the same group by fractional crystallization of the phenocryst phases in these volcanics [4,6,9,15 and references therein], suggesting that assimilation during fractional crystallization (AFC) may control the isotopic variations between primitive and evolved compositions. Correlation between differentiation parameters, such as Mg#, and isotopic ratios (Fig. 8) strongly supports AFC for the Pliocene volcanics. Furthermore, the isotopic differences between the Pliocene mafic and evolved volcanics cannot reflect a uni-directional temporal variation in the source composition, since these volcanics are intercalated (see Table 1 and Fig. 10). Although the Miocene evolved and primitive mafic volcanics are not intercalated, the similar correlations between isotopic and major element composition between the Miocene and Pliocene–Recent volcanics are consistent with a similar process controlling both trends.

5.2.2. Location of assimilation: crust or mantle?

The depths at which assimilation occurred can provide important information about the isotopic composition of the lithosphere beneath Gran Canaria. Of primary importance is whether assimilation occurred within the crust or mantle. Several arguments favor assimilation of mantle-derived melts. First, the crust does not have the appropriate isotopic composition to serve as the SEV or EV endmember. The crust beneath Gran Canaria consists of three components: (1) a 5–10 km thick wedge of sediments from the African continental rise; (2) igneous oceanic crust; and (3) the submarine volcanic pile and intrusives associated with earlier Canary volcanism [7]. As pointed out by Sun [18] and Cousens et al. [6], the Gran

Canaria volcanics show no evidence for sediment assimilation on the $^{206}\text{Pb}/^{204}\text{Pb}$ versus $^{207}\text{Pb}/^{204}\text{Pb}$ diagram (Fig. 5; see also sediment data in Table 1). If significant sediment assimilation had occurred, the Miocene and Pliocene–Recent groups would have formed trends with negative or nearly vertical not horizontal to slightly positive slopes. In addition, Ce/Pb and Nb/U ratios show no systematic variation with Mg# for samples with Mg# > 50 (Ce and Nb data from Hoernle and Schmincke [4]). These ratios are much higher (25–70 and 25–100, respectively) than in continental crust (4 and 10, respectively [22]), or than Ce/Pb in sediments from DSDP site 397 [3–7; Hoernle, unpublished data]. Although the isotopic composition of the igneous portion of the oceanic crust beneath Gran Canaria has not been determined, a gabbro xenolith from Lanzarote has a very high $^{143}\text{Nd}/^{144}\text{Nd}$ ratio and a low $^{87}\text{Sr}/^{86}\text{Sr}$ ratio (see discussion below) [2], suggesting that the igneous portion of the crust beneath the eastern Canary Islands is isotopically similar to MORB. The $^{143}\text{Nd}/^{144}\text{Nd}$ ratios in Recent Atlantic MORB [23], Jurassic Atlantic MORB at the Cape Verde Islands [20] and the gabbro xenolith are > 0.5130. Since seawater alteration will not significantly affect the $^{143}\text{Nd}/^{144}\text{Nd}$ ratio, assimilation of either fresh- or seawater-altered igneous oceanic crust would cause an increase in the $^{143}\text{Nd}/^{144}\text{Nd}$ ratio and thus cannot explain the Miocene or Pliocene–Recent trends at Gran Canaria. Lower continental crustal material such as granulites could have the appropriate isotopic composition to serve as an endmember for the Pliocene trend and could have been dismembered and included in the igneous crust during rifting. Lower continental crustal xenoliths, however, have never been found on Gran Canaria, and there is no seismic evidence for lower continental crustal material beneath Gran Canaria [8]. Although the composition of the early Gran Canaria magmas is not known, the complete history of the neighboring island of Fuerteventura, from the inception of volcanism in the Cretaceous to the present, is subaerially exposed [11]. Neither the Miocene–Cretaceous volcanics and intrusives (> 21 Ma) [16], nor their hydrothermally altered products (seawater alteration = increase in $^{87}\text{Sr}/^{86}\text{Sr}$), could serve as an appropriate endmember for the SEV or EV.

The second argument for assimilation occurring in the lithospheric mantle involves evidence for the depth of fractional crystallization. Seismic studies indicate that the boundary between the oceanic crust and the upper mantle (or the depth of the Moho) beneath Gran Canaria is at approximately 13–14 km [8]. Based on the presence of olivine and clinopyroxene but the absence of plagioclase on the liquidus for most Pliocene basalts with $Mg\# > 50$, crystal fractionation within these basalts probably occurred at depths in excess of 15 km [4]. We note, however, that the relevant experimental data only strictly applies to the moderately undersaturated compositions. Since most of the change in isotopic composition for a given age group occurs within basalts with $Mg\# > 50$ (Fig. 8), assimilation within at least the moderately undersaturated basalts must have occurred within the lithospheric mantle. SiO_2 -undersaturated evolved volcanics, even highly undersaturated and evolved phonolitic compositions, commonly contain lherzolitic xenoliths, indicating that highly undersaturated magmas also commonly fractionate within the mantle [24]. Pliocene volcanics with $Mg\# < 50$ probably cooled and fractionated within the crust based on the presence of plagioclase on the liquidus for these samples [4]. In contrast to the Pliocene volcanics with $Mg\# > 50$, the volcanics with $Mg\# < 50$ plot on the 1 bar cotectics in the projection from plagioclase onto the Ol-Di-Neph triangle of Sack et al. [25]. The lack of isotopic variation with $Mg\#$ (Fig. 8) or with other differentiation parameters for these volcanics suggests that (1) they crystallized within well-insulated chambers or (2) the wall rocks were significantly depleted in low-temperature melting components so that assimilation was not detectable, as might be the case with unaltered, igneous oceanic crust.

A third argument for assimilation occurring in the mantle instead of the crust is based on evidence for the presence of enriched mantle beneath the eastern Canary Islands. (1) The saturated primitive basalts from both age groups on Gran Canaria are shifted toward the evolved endmembers. It is unlikely that basalts with $Mg\# > 62$ have experienced noticeable crustal contamination. (2) Sövitic carbonatites from the neighboring island of Fuerteventura have similar isotopic compositions to the SPV and evolved groups on Gran

Canaria [16]. Not only do the carbonatites have mantle oxygen and carbon isotopic compositions, but it is unlikely that the Sr and Nd isotope ratios of carbonatites will be affected by crustal contamination, due to their extremely high concentrations of Sr and Nd. (3) St. Paul's Rocks, a piece of mantle peridotite subaerially exposed in the mid Atlantic Ocean, has the appropriate isotopic composition to serve as the Miocene SEV component in Figs. 4, 6 and 7.

Taken together, the above arguments strongly support the hypothesis that isotopically enriched (relative to MORB or DM) material is present in the shallow (probably lithospheric) mantle beneath Gran Canaria, and perhaps beneath the other eastern Canary Islands [16]. Similar arguments can also be extended to coexisting suites of mafic and evolved volcanics from other ocean islands. For example, compared to the associated mafic volcanics, the evolved volcanics from the Pico de Antonio Formation on São Tiago, Cape Verde Islands are shifted in a similar direction as the evolved Pliocene–Recent volcanics. The differences in isotopic composition between the mafic and evolved volcanics on São Tiago are consistent with enriched material in the lithospheric mantle beneath the southeastern Cape Verdes [20].

Xenoliths provide an additional method for determining the composition of crustal and mantle rocks beneath ocean islands. Vance et al. [2] report five Sr and Nd isotope analyses of xenoliths from the Canary Islands. Three of the xenoliths—a spinel lherzolite, a gabbro and a dunite—are from recent basalts on Lanzarote. Two other xenoliths—a harzburgite and a hornblende clinopyroxenite—are probably from < 2.7 Ma nephelinite flows on Gran Canaria. The gabbro sample has an extremely high $^{143}Nd/^{144}Nd$ ratio (0.51333) and a fairly low $^{87}Sr/^{86}Sr$ ratio (0.70297), similar to seawater-altered MORB, and suggests that the oceanic crust beneath Lanzarote has a MORB-like composition. The other four xenoliths have isotopic compositions which as a group are distinct from MORB but indistinguishable within analytical error from the Canary Island volcanics [2]. Although the dunite and hornblende clinopyroxenite are probably cumulates from Canary magmas [15,26], the spinel lherzolite and harzburgite probably represent pieces of the preexisting mantle beneath the Canary Islands. Only one xenolith,

a harzburgite from Lanzarote, has been analyzed for Pb isotopes [27]. The Pb isotopic composition is similar to that found in evolved Pliocene volcanics (6/4, 7/4, 8/4: 18.9, 15.56, 38.9). If these xenoliths did not re-equilibrate with their host basalts and were not contaminated by earlier plume-derived magmas, they may provide additional evidence for isotopically enriched mantle beneath the eastern Canary Islands.

5.2.3. Evidence for a heterogeneous lithospheric mantle

In all isotope correlation diagrams, the saturated primitive and the evolved compositions are shifted towards enriched mantle (EM). The Pliocene EV component could have a composition similar to EM1 in all isotope correlation diagrams (Figs. 4–7). The Miocene volcanics form similar trends to the Pliocene volcanics in all isotope correlation diagrams except those with Nd. The non-variant $^{143}\text{Nd}/^{144}\text{Nd}$ ratios of the Miocene volcanics, which are analytically indistinguishable from the average value of the western Canary Islands, suggest that either (1) the Nd isotopes were not significantly affected by assimilation, or (2) the assimilant had an identical Nd isotopic composition [6]. Assuming the first possibility, an important question is whether the Miocene and Pliocene assimilants had similar isotopic compositions. If this were the case, then both the Sr/Nd and the Pb/Nd ratios of the Miocene volcanics should be substantially lower than of the Pliocene volcanics. Comparing these ratios in the SPV (to avoid possible changes in these ratios due to fractional crystallization), the Miocene SPV have lower Sr/Nd (9.1–11.9) than the Pliocene–Recent SPV (15.1–19.9) but similar Pb/Nd (0.049–0.056 and 0.036–0.084, respectively). The observed Pb/Nd ratios are inconsistent with the hypothesis that the Miocene and Pliocene assimilants had similar isotopic compositions, indicating heterogeneity in the lithospheric mantle beneath Gran Canaria. Nevertheless, it is unlikely in a heterogeneous lithosphere that all of the Miocene assimilants would have had identical Nd isotopic compositions and that their Nd isotopic compositions would have been identical to the most plume-like melts (UV). For these reasons, we prefer the interpretation that the Miocene Nd isotopic compositions were not affected by lithospheric contamination. There-

fore, the composition of the Miocene SEV component may have been similar to EM2 (Figs. 4–7). It is important to note, however, that even if the Nd isotopes have been unaffected by assimilation, the composition of the SEV component cannot be identical to that of the Zindler and Hart [1] EM2 component. Since two component mixing on the $^{206}\text{Pb}/^{204}\text{Pb}$ versus $^{207}\text{Pb}/^{204}\text{Pb}$ diagram will form a linear mixing array, assimilation of the Zindler and Hart EM2 component by melts with compositions similar to the Miocene UV would have resulted in trends with negative rather than with no or slightly positive slopes (Fig. 5).

Since it appears that the Miocene and Pliocene melts assimilated components with different isotopic compositions, the next question concerns the location of these EM1- and EM2-like components in the lithospheric mantle. Several factors suggest that the Miocene magmas may have been contaminated at greater depths than the Pliocene magmas. After the > 3 Myr hiatus in volcanic activity that followed the Miocene Cycle of volcanism, the early Pliocene magmas probably had to establish a new plumbing system. Since the Pliocene central eruption complex, from which most of the SPV and EV were erupted during stages 2 and 3, was located within the Miocene caldera, the Pliocene plumbing network was most likely intertwined with the frozen Miocene conduits and chambers. It is therefore unlikely that lateral separation of EM1- and EM2-like components in the lithospheric mantle can alone explain the distinct Miocene and Pliocene–Recent trends in isotope correlation diagrams.

The maximum deviation from the isotopic composition of the plume and asthenosphere, which have compositions most similar to the UV and the UPV, respectively, occurred during stage 3 of each cycle. Pliocene stage 3 evolved volcanics are intercalated with primitive ($\text{Mg}\# > 62$) basalts, which have different isotopic compositions. Since the basalts and evolved rocks can be related through fractional crystallization at moderate pressures, assimilation must have occurred at shallow depth within the lithospheric mantle. Major element data from the Pliocene SPV indicates that most of these basalts fractionated olivine \pm clinopyroxene at depths shallower than ~ 60 km [4], also consistent with assimilation of upper lithospheric mantle. We propose therefore that the EM1-like component

beneath Gran Canaria is located in the upper part of the lithospheric mantle.

Since no primitive basalts are intercalated with the Miocene SEV, the change in isotopic composition between the primitive basalts in stage 2 and the evolved volcanics in stage 3 could reflect either assimilation (1) within the lower lithosphere, in which case the primitive (but not primary) basalts and the evolved volcanics could have had the same composition, or (2) within the upper lithospheric mantle, in which case the primitive basalts and evolved volcanics would have had different compositions. Since there are arguments for placing the EM1-like material in the upper lithospheric mantle and there are no arguments *against* placing the EM2-like material in the lower lithosphere, we propose that the EM2-like component is located in the lower lithosphere beneath Gran Canaria. A recent study of a Hawaiian xenolith, which contains cumulus spinel and olivine and intercumulus garnet, suggests that Hawaiian shield stage magmas (roughly equivalent to Miocene stage 2) may pond and fractionate in the lower lithosphere before ascending to the surface [28]. If the Miocene stage 2 and 3 magmas resided in lower lithospheric reservoirs, their compositional differences may reflect longer residence times (and thus larger amounts of assimilation) of the stage 3 magmas in the lower lithosphere, resulting from a decline in magma supply to the already established reservoirs.

5.3. Origin of the lithosphere, asthenosphere and plume material beneath Gran Canaria

Enriched mantle (EM1 and EM2) is characteristic of ultramafic xenoliths from ancient continental lithospheric mantle [29,30]. The EM1 component is characteristic of mafic magmas, megacrysts or ultramafic xenoliths from Archean continental lithospheric mantle, such as, the Smoky Butte lamproites from Montana (USA), the Loch Roag xenoliths from Scotland or the inclusions in diamonds from South Africa. The EM2 component is characteristic of Proterozoic continental lithospheric mantle and appears to be related to enrichments occurring above subducting slabs. Continental lithospheric mantle can be incorporated into the asthenosphere and/or oceanic lithosphere by delamination and/or thermal erosion

during rifting [20,21,31,32]. We propose that, during the break-up of Pangaea and subsequent rifting, parts of the continental lithospheric mantle beneath the West African Craton were incorporated into the asthenosphere and subsequently into the oceanic lithospheric mantle beneath at least some of the Canary and Cape Verde Islands [20]. In addition to the ocean island volcanics, Jurassic MORB basalts from the Cape Verde Islands may also provide additional evidence for the presence of EM material in the asthenosphere during the rifting of Pangaea. Although it is difficult to determine the initial Sr and Pb isotopic compositions of these seawater-altered basalts, the estimated initial $^{143}\text{Nd}/^{144}\text{Nd}$ isotopic compositions range from 0.51282 to 8 [20]. These values are significantly lower than observed in recent Atlantic MORB, which have values > 0.51299 [23], possibly reflecting the presence of enriched continental lithospheric mantle in the Jurassic MORB source. The above evidence from the Canary and Cape Verde Islands, the composition of St. Paul's Rocks [19], and possibly the isotopic composition of mantle xenoliths from ocean islands [2,33,34] suggest that enriched material may be common in the upper mantle beneath ocean basins, consistent with the proposal of Hawkesworth et al. [32] for a shallow origin of the DUPAL (cf. [17]) anomaly.

Most of the isotopic data from Atlantic ocean islands, especially those above 18°S latitude, require involvement of a HIMU component. The most widely accepted origin for the HIMU component is recycled, altered oceanic crust (e.g. [35,36]). There has been considerable debate, however, as to why subducted crust should have a high U/Pb (or Mu) ratio. Recent data from mantle xenoliths [37] suggest that U may be more compatible in clinopyroxene than Th and Pb. Since U and Sr are also more compatible than Rb, and Sm is more compatible than Nd, clinopyroxene—given sufficient time—could evolve to a HIMU-like composition. One of the major sources of clinopyroxene in the mantle is subducted crust. Since sediments, which are concentrated on the top of the subducting slab, will probably melt and separate from the subducting slab at shallow depths, clinopyroxene may control the isotopic composition of deeply subducted crustal material. We propose that blobs of subducted crust, upwelling

from the upper mantle–lower mantle or the lower mantle–core boundary, may be the source of the HIMU component in some ocean island volcanics.

6. A dynamic model for the isotopic evolution of Gran Canaria

At least two cycles of volcanism are subaerially exposed on Gran Canaria. Below we compare and contrast the isotopic evolution of these two cycles, in the context of a “blob” model proposed for the Canary Islands by Hoernle and Schmincke [5]. During the Miocene, a blob of HIMU-like material ascended through the asthenosphere until it encountered the base of the lithosphere beneath Gran Canaria. During its ascent, the blob may have entrained asthenospheric material with a DM-like (= DM + minor EM) composition (Fig. 11). This blob formed the Miocene or Shield Cycle of volcanism on Gran Canaria. Although Miocene stage 1 is not exposed on Gran Canaria, the early history of the Shield Cycle on Gran Canaria is inferred from the neighboring island of Fuerteventura. Low-degree, SiO₂-undersaturated melts with HIMU-like compositions formed in the cooler, upper rim of the blob [16] by decompression melting. These magmas interacted with the lithospheric mantle, assimilating melts with enriched (EM-like) compositions.

During stage 2, the center of the blob reached the base of the lithosphere. Large degrees of melting in the hot core of the blob formed large volumes of SiO₂-saturated (picritic) melts, which initially had HIMU-like compositions, similar to the more undersaturated melts. Transfer of heat from the blob to the base of the lithosphere raised the isotherms in the base of the lithosphere, causing melting of the lower lithosphere (see Fig. 11) [20,38]. Large chambers for storing these voluminous picritic melts may have formed at the base or within the lowermost lithosphere at this time [28,38]. Assimilation of lower lithospheric material, shifted the composition of the stage 2 melts toward an enriched (EM2-like) composition. A well-insulated magma plumbing system may have been developed in the upper lithosphere during stage 1 and possibly during early stage 2, so that the later magmas were shielded from upper lithospheric contamination.

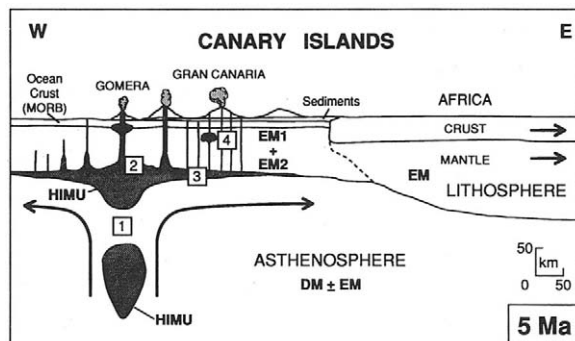


Fig. 11. Hypothetical cross-section through the Canary Islands at 5 Ma illustrating the isotopic composition of the plume (HIMU-like), asthenosphere (DM + EM = a composition similar to E-MORB), upper lithospheric mantle (EM1-like) and lower lithospheric mantle (EM2-like) beneath the Canary Islands. The numbers indicate the locations where various Gran Canaria magmas (or source material) may have been contaminated. During ascent (location 1), the HIMU plume (or blobs [5]) may have entrained asthenospheric material, resulting in a composition similar to the Miocene UV (stage 4 volcanics). Melting and assimilation of lower lithosphere above the plume (location 2), when the island is in its shield cycle, could explain the composition of the Miocene SPV and SEV (stage 2 and 3 volcanics). As plume material spreads out along the base of the lithosphere (location 3), preferentially in the direction of asthenospheric flow or towards the older volcanoes, additional entrainment of asthenospheric material and interaction with the base of the lithosphere may yield a composition similar to the Pliocene–Recent UPV (stage 1 and 4 volcanics). Assimilation of upper lithospheric mantle (location 4) by melts from the rejuvenated stages could result in compositions similar to the Pliocene SPV and EV (stage 2 and 3 volcanics). The enriched mantle in the lithosphere and asthenosphere beneath the eastern Canary Islands may reflect recycling of West African lithospheric mantle during the rifting of Pangaea.

During stage 3, the cooler, lower rim of the blob began to replace the core at the base of the lithosphere. As the magma production rate decreased, melts resided in the lower lithospheric chambers for longer periods, initially assimilating greater amounts of lower lithospheric material so that these melts had the most EM2-like compositions (SEV endmember). As the lower rim of the blob continued to replace the core material, heat transfer to the base of the lithosphere diminished. Lowering of the isotherms and depletion of enriched material in the lower lithosphere was accompanied by a systematic decrease in melting and assimilation of the lower lithosphere by the blob melts at the end of stage 3. Miocene stage 4 volcanics assimilated the least amount of lower

lithosphere and thus have isotopic compositions that most closely reflect the HIMU-like composition of the plume (\pm entrained DM-like material from the asthenosphere: UV endmember).

In the late Miocene, another blob reached the base of the lithosphere to the west of Gran Canaria, beneath the neighboring islands of Tenerife and la Gomera (Fig. 1). This blob formed the shield Cycle of volcanism on la Gomera and possibly Tenerife and a rejuvenated (i.e. Pliocene) cycle on Gran Canaria. After contacting the base of the lithosphere beneath la Gomera and Tenerife, blob material, which still contained fusible material or unsegregated melts, spread through the upper asthenosphere along the base of the lithosphere [38,39]. En route to the base of the lithosphere beneath Gran Canaria, the blob material (and/or melts) entrained upper asthenospheric (and possibly lower lithospheric) components with DM-like compositions [40].

The geochemical evolution of the Pliocene Cycle on Gran Canaria—from highly undersaturated, to saturated, and back to highly undersaturated compositions (similar to that of the Miocene Cycle)—reflected passage of rim-core-rim material of the Pliocene Blob beneath Gran Canaria. During Pliocene-Recent Stages 1 and 4, low-degree, highly undersaturated, volatile-rich melts segregated from what had been the rim of the ascending Pliocene Blob. The isotopic composition of these melts represents a mix of HIMU-like blob material and DM-like asthenospheric material (UPV endmember). In contrast to the evolved stage 1 volcanics from the shield cycle on Fuerteventura, which show evidence of lithospheric contamination [16], the primitive rejuvenated Stage 1 volcanics on Gran Canaria show little evidence of lithospheric interaction. Wyllie [38] proposed that “Crack propagation may be favored in lithosphere that has previously provided conduits to the surface.” Explosive crack propagation may facilitate the rapid ascent of magmas from the asthenosphere-lithosphere boundary to the surface [38,41], explaining why rejuvenated stage 1 magmas have primitive compositions and show little lithospheric interaction.

In contrast to Miocene Stage 2 and 3 volcanics on Gran Canaria, the Pliocene Stage 2 and 3 volcanics only show evidence of contamination by EM1-like upper lithospheric mantle (EV endmem-

ber). Two reasons for the lack of evidence of lower lithospheric contamination are as follows. First, during the Miocene, most of the lowermost lithosphere was probably replaced by residual Miocene Blob (HIMU-like) and asthenospheric (DM-like) material. Second, the volume and temperature of the blob material that passed beneath Gran Canaria during the Pliocene was significantly lower than in the Miocene. Melting of the lower lithosphere and contamination of asthenospheric melts therefore were probably not as significant in the Pliocene. On the other hand, due to the substantially lower magma production and thus lower supply rates, the conduit and magma storage network for the Pliocene magmas never became as well established and never reached the degree of chemical and thermal equilibrium with the ascending Pliocene melts as did the Miocene plumbing network. As a result, upper lithospheric contamination may be more prevalent in the rejuvenated cycles than in shield cycles. If the Quaternary volcanism represents the beginning of a new cycle, it will most likely evolve in a manner more similar to the Pliocene than to the Miocene Cycle of volcanism.

7. Summary and conclusions

Mixing of four components can explain the range in isotopic composition of the volcanics from Gran Canaria, which span the entire ~ 15 Myr subaerial volcanic history of the island. The Miocene (~ 9 – 15 Ma) and the Pliocene-Recent (~ 0 – 5.5 Ma) volcanics form distinct trends in isotope correlation diagrams. The most SiO_2 -undersaturated volcanics from both age groups have the least radiogenic Sr and the most radiogenic Pb; the most SiO_2 -undersaturated volcanics from the Pliocene-Recent also have the most radiogenic Nd. The Pliocene-Recent undersaturated group has less radiogenic Pb than the Miocene undersaturated group. Both of the most undersaturated groups overlap the field for the western Canary Islands, which presently overlie the Canary Plume. Compared to the most SiO_2 -undersaturated volcanics, evolved volcanics from both age groups extend to more radiogenic Sr and less radiogenic Nd (for Pliocene-Recent volcanics only) and Pb; the most SiO_2 -saturated primitive basalts from each group extend to intermediate

compositions. There is no evidence that any of the Gran Canaria volcanics were significantly contaminated in the crust. All available evidence suggests that the four Gran Canaria components were located within the mantle.

We propose that the observed isotopic variations reflect interaction between plumes (or blobs) with the asthenosphere and lithospheric mantle beneath Gran Canaria. The most undersaturated Miocene volcanics are closest in composition to the Canary Plume (HIMU-like). The more saturated primitive Miocene basalts and their differentiates, erupted in the middle of the Miocene Cycle of volcanism when the plume was directly beneath Gran Canaria, may have assimilated lower lithosphere (EM2-like). During the Pliocene–Recent epochs, the Canary Plume was situated to the west of Gran Canaria. The shift towards less radiogenic Pb of the most undersaturated Pliocene–Recent basalts, as compared to the most undersaturated Miocene volcanics, may reflect greater entrainment of asthenospheric material (having a DM-like composition = DM + minor EM) as plume material or melt was transported through the upper asthenosphere to the base of the lithosphere beneath Gran Canaria. Since the base of the lithosphere beneath Gran Canaria was depleted and partially replaced by residual plume and asthenospheric material during the Miocene, the most-saturated Pliocene basalts and evolved volcanics primarily assimilated upper lithospheric material (EM1-like).

Evidence presented in this study for enriched material (EM1 and EM2) in the lithospheric mantle beneath at least some of the Canary and Cape Verde Islands is consistent with a shallow (upper mantle) origin for the DUPAL anomaly [32]. The study also suggests that HIMU-like material may be derived from deeper sources, which implies separate mantle histories for the EM and HIMU components.

Acknowledgements

This study represents part of a Ph.D. dissertation by K.H. We are grateful to David Graham, Brian Cousens, Frank Spera and Jim Mattinson for reviewing this manuscript and for stimulating discussions. Dave Clague, Fred Frey and an unknown reviewer are thanked for their extensive

comments which greatly improved the manuscript. The research was in part supported by NSF grant EAR88-17802 to GRT. The sediment samples came from the Lamont-Doherty Geological Observatory DSDP core collection.

References

- 1 A. Zindler and S.R. Hart, Chemical geodynamics, *Ann. Rev. Earth Planet. Sci.* 14, 493–571, 1986.
- 2 D.J. Vance, J.O.H. Stone and R.K. O’Nions, He, Sr and Nd isotopes in xenoliths from Hawaii and other oceanic islands, *Earth Planet. Sci. Lett.* 96, 147–160, 1989.
- 3 K. Hoernle, The major element, trace element and Sr-Nd-Pb isotopic evolution of Gran Canaria (Canary Islands) magma sources over the past 15 Myr: Inferences on the geochemical and structural evolution of the mantle. Ph.D. dissertation, University of California, Santa Barbara, 140 pp., 1990.
- 4 K. Hoernle and H.-U. Schmincke, The Major and trace element geochemistry of the tholeiite-melilite nephelinite basalts on Gran Canaria, Canary Islands: Crystal fractionation, accumulation and melting depth, *J. Petrol.*, in press.
- 5 K. Hoernle and H.-U. Schmincke, The major and trace element evolution of Gran Canaria magma sources over the past 15 Myr: an intermittent Canary Island Plume?, *J. Petrol.*, in press.
- 6 B.L. Cousens, F.J. Spera and G.R. Tilton, Isotopic patterns in silicic ignimbrites and lava flows of the Mogan and lower Fataga Formations, Gran Canaria, Canary Islands: temporal changes in mantle source composition, *Earth Planet. Sci. Lett.* 96, 319–335, 1990.
- 7 U. Von Rad, K. Hinz, M. Sarnthein and E. Seibold, *Geology of the Northwest African Continental Margin*, 703 pp., Springer-Verlag, New York, N.Y., 1982.
- 8 E. Banda, J.J. Danobeitia, E. Surinach and J. Ansorge, Features of crustal structure under the Canary Islands, *Earth Planet. Sci. Lett.* 55, 11–24, 1981.
- 9 H.-U. Schmincke, Volcanic and chemical evolution of the Canary Islands, in: *Geology of the Northwest African margin*, U. von Rad, K. Hinz, M. Sarnthein and E. Seibold, eds., pp. 273–306, Springer-Verlag, New York, N.Y., 1982.
- 10 I. McDougall and H.U. Schmincke, Geochronology of Gran Canaria, Canary Islands: Age of shield building volcanism and other magmatic phases, *Bull. Volcanol.* 40, 1–21, 1976.
- 11 M.J. Le Bas, D.C. Rex and C.J. Stillman, The early magmatic chronology of Fuerteventura, Canary Islands, *Geol. Mag.* 123(3), 287–298, 1986.
- 12 J.B. Minister and T.H. Jordan, Present day plate motions: a summary, in: *Source Mechanisms and Earthquake Prediction*, C.J. Allégre., ed., pp. 109–124, Editions du Centre National de la Recherche Scientifique, Paris, 1980.
- 13 R.A. Duncan, Hotspots in the southern oceans—an absolute frame of reference for the motion of the Gondwana continents, *Tectonophysics* 74, 29–42, 1981.
- 14 W.J. Morgan, Hotspot tracks and the early rifting of the Atlantic, *Tectonophysics* 94, 123–139, 1983.

- 15 K. Hoernle, General geology and petrology of the Roque Nublo volcanics on Gran Canaria, Canary Islands, Spain. M.A. thesis, University of California, Santa Barbara, 191 pp., 1987.
- 16 K. Hoernle and G.R. Tilton, Sr-Nd-Pb isotope data for Fuerteventura (Canary Islands) basal complex and sub-aerial volcanics: applications to magma genesis and evolution, *Schweiz. Mineral. Petrogr. Mitt.* 71, 5–21, 1991.
- 17 S.R. Hart, A large-scale isotope anomaly in the southern hemisphere mantle, *Nature* 309, 753–757, 1984.
- 18 S.S. Sun, Lead isotopic study of young volcanic rocks from mid-ocean ridges, ocean islands and island arcs, *Philos. Trans. R. Soc. London Ser. A* 297, 409–445, 1980.
- 19 M.K. Roden, S.R. Hart, F.A. Frey and W.G. Melson, Sr, Nd, and Pb isotopic and REE geochemistry of St. Paul's Rocks, the metamorphic and metasomatic development of an alkali basalt mantle source, *Contrib. Mineral. Petrol.* 85, 376–390, 1984.
- 20 D.C. Gerlach, R.A. Cliff, G.R. Davies, M. Norry and N. Hodgson, Magma sources of the Cape Verdes archipelago: Isotopic and trace element constraints, *Geochim. Cosmochim. Acta* 52, 2979–2992, 1988.
- 21 D.C. Gerlach, J.C. Stormer, Jr. and P.A. Mueller, Isotopic geochemistry of Fernando de Noronha. *Earth Planet. Sci. Lett.* 85, 129–144, 1987.
- 22 A.W. Hofmann, K.P. Jochum, M. Seufert and W.M. White, Nb and Pb in oceanic basalts: New constraints on mantle evolution, *Earth Planet. Sci. Lett.* 79, 33–45, 1986.
- 23 E. Ito, W.M. White and C. Göpel, The O, Sr, Nd and Pb isotope geochemistry of MORB, *Chem. Geol.* 62: 157–176, 1987.
- 24 A.J. Irving and R.C. Price, Geochemistry and evolution of lherzolite-bearing phonolitic lavas from Nigeria, Australia, East Germany and New Zealand, *Geochim. Cosmochim. Acta* 48, 1201–1221, 1981.
- 25 R.O. Sack, D. Walker and I.S.E. Carmichael, Experimental petrology of alkalic lavas: constraints on cotectics of multiple saturation in natural basic liquids, *Contrib. Mineral. Petrol.* 96, 1–23, 1987.
- 26 T. Frisch and H.-U. Schmincke, Petrology of clinopyroxene-amphibole inclusions from the Roque Nublo Volcanics, Gran Canaria, Canary Islands (Petrology of Roque Nublo Volcanics I), *Bull. Volcanol.* 33, 1073–1088, 1969.
- 27 R.E. Zartman and F. Tera, Lead concentration and isotopic composition in five peridotite inclusions of probable mantle origin, *Earth Planet. Sci. Lett.* 20, 54–66, 1973.
- 28 G. Sen and R.E. Jones, Cumulate Xenolith in Oahu, Hawaii: implications for deep magma chambers and Hawaiian volcanism, *Science* 249, 1154–1157, 1990.
- 29 M.A. Menzies, Cratonic, circum-cratonic and oceanic mantle domains beneath the western U.S.A., *J. Geophys. Res.* 94(B6), 7899–7915, 1989.
- 30 C.J. Hawkesworth, P.D. Kempton, N.W. Rogers, R.M. Ellam and P.W. van Calsteren, Continental mantle lithosphere, and shallow level enrichment processes in the Earth's mantle, *Earth Planet. Sci. Lett.* 96, 256–268, 1990.
- 31 D. McKenzie and R.K. O'Nions, Mantle reservoirs and ocean island basalts, *Nature* 301, 229–231, 1982.
- 32 C.J. Hawkesworth, M.S.M. Mantovani, P.N. Taylor and Z. Palacz, Evidence from the Parana of South Brazil for a continental contribution to DUPAL basalts, *Nature* 322, 356–359, 1986.
- 33 Q. Cheng, J. Natland and J.D. MacDougall, Extensively melted enriched lithosphere in the SW Pacific—evidence from Samoan and Tahitian ultramafic xenoliths, *EOS Trans. Geophys. Soc. Am. (Abstr.)* 69(44), 1500, 1988.
- 34 M. Brouxel and M. Tatsumoto, Sr, Nd, and Pb isotopes of spinel lherzolite xenoliths, Koloa Volcanics, Kauai, Hawaii, *EOS Trans. Geophys. Soc. Am. (Abstr.)* 69(44), 1517, 1988.
- 35 A.W. Hofmann and W.H. White, Mantle plumes from ancient oceanic crust, *Earth Planet. Sci. Lett.* 57, 421–436, 1982.
- 36 A. Zindler, E. Jagoutz and S. Goldstein, Nd, Sr and Pb isotopic systematics in a three-component mantle: a new perspective, *Nature* 298, 519–523, 1982.
- 37 A. Meijer, T.T. Kwon and G.R. Tilton, U-Th-Pb partitioning behavior during partial melting in the upper mantle: implications for the origin of high mu components and the "Pb paradox," *J. Geophys. Res.* 95 (B1), 433–448, 1990.
- 38 P.J. Wyllie, Solidus curves, mantle plumes, and magma generation beneath Hawaii. *J. Geophys. Res.* 93(B5), 4171–4181, 1988.
- 39 P. Olsen, G. Schubert, C. Anderson and P. Goldman, Plume formation and lithosphere erosion: a comparison of laboratory and numerical experiments, *J. Geophys. Res.* 93, 15,065–15,084, 1988.
- 40 R.W. Griffiths, The differing effects of compositional and thermal buoyancies on the evolution of mantle diapirs, *Phys. Earth Planet. Inter.* 43, 261–273, 1986.
- 41 F.J. Spera, Carbon dioxide in petrogenesis, III, role of volatiles in the ascent of alkaline magma with special reference to xenolith-bearing mafic lavas, *Contrib. Mineral. Petrol.* 88, 217–232, 1984.
- 42 H.-U. Schmincke, *Geological Field Guide of Gran Canaria*, 4th ed., 212 pp., Pluto Press, Witten, 1990.
- 43 W. Todt, R.A. Cliff, A. Hanser and A.W. Hofmann, ²⁰²Pb-²⁰⁵Pb spike for Pb isotopic analysis, *Terra Cognita* 4, 209, 1984.